Soft Matter

Cite this: *Soft Matter*, 2011, **7**, 1644

www.rsc.org/softmatter

COMMUNICATION

A membrane fusion assay based on pore-spanning lipid bilayers†

Ines Höfer and Claudia Steinem*

Received 6th December 2010, Accepted 4th January 2011
DOI: 10.1039/c0sm01429j

Pore-spanning planar membranes on highly ordered porous silicon substrates were shown to be well suited to monitor the calcium ion mediated fusion of large unilamellar vesicles by means of confocal laser scanning fluorescence microscopy and scanning ion conductance microscopy in real-time.

Fusion of lipid membranes plays a central role in many biological processes. For example, in the case of synaptic transmission, fusion is a fundamental event that is tightly regulated by a number of proteins of which SNAREs have been shown to play a crucial role.[1] In an effort to understand the molecular mechanism of fusion, a variety of *in vitro* fusion assays has been developed to monitor the different steps that occur during this process.[2–6] It has been proposed that after first docking of the bilayers, an intermediate, hemifused state is adopted, in which the outer leaflets have merged, but the inner leaflets and contents remain distinct.[7] A transition into full fusion then involves mixing of both leaflets and content exchange. While established *in vitro* vesicle–vesicle fusion assays are essentially bulk measurements with a few exceptions,[8,9] the application of planar membranes such as black lipid membranes (BLMs) and solid supported membranes (SSMs) allows for the detection of single fusion events with high time resolution.[10–17] However, BLMs are not very robust and experiments lack reproducibility.[3] Moreover, BLM preparations prevent the adjustment of defined protein densities, which is a prerequisite for addressing open questions in SNARE-mediated fusion. In contrast, SSMs are robust and long-term stable.[6,10,18] However, in this case the bilayer is in close contact to the substrate, and hence it is not accessible from both sides limiting the observation of content release and fusion pore formation as well as the addition of fusion modulating compounds or the application of transmembrane potentials.

Herein, we present a new and versatile fusion assay based on pore-spanning membranes that can overcome the drawbacks of BLMs and SSMs (Fig. 1). Pore-spanning membranes are proven to be mechanically robust and long-term stable.[19–21] As they are deposited on an open pore array, both sides can be addressed individually allowing the application of a transmembrane potential, fusion modulating compounds and an electrochemical gradient. As shown recently, pore-spanning membranes obtained from vesicle spreading and fusion can even be doped with a high number of proteins.[22,23]

In this study, we made use of pore-spanning membranes that are obtained by the painting technique,[24] which are termed micro-BLMs. Micro-BLMs composed of 1,2-diphythanoyl-*sn*-glycero-3-phosphocholine (DPhPC)/1-palmitoyl-2-oleoyl-*sn*-glycero-3-phosphoethanolamine (POPE) (2 : 1) doped with 1 mol% Oregon Green DHPE were formed on gold covered highly ordered porous silicon substrates with pore diameters of 1.2 μm. To render the upper surface hydrophobic, the gold surface was functionalized with 1,2-dipalmitoyl-*sn*-glycero-3-phosphothioethanol (DPPTE). After adding a small droplet of DPhPC/POPE (2 : 1) dissolved in *n*-decane on the hydrophobic porous substrate, pore-spanning membranes are obtained, in which a lipid bilayer is formed across the pores, while a hybrid layer is formed on the pore rims. The formation of the micro-BLMs was followed by means of an upright confocal laser scanning fluorescence microscope (CLSM). A preparation is called successful, if the green fluorescence of the Oregon Green DHPE doped pore-spanning membranes is observed, while the fluorescence is quenched on the gold covered pore-rims, which thus appear black (Fig. 2, top panel).

To these micro-BLMs, large unilamellar vesicles (LUVs) composed of 1-palmitoyl-2-oleoyl-*sn*-glycero-3-phosphocholine (POPC)/1-palmitoyl-2-oleoyl-*sn*-glycero-3-phosphoserine (POPS) (4 : 1) with a mean diameter of 600 nm[23] doped with 1 mol% Texas Red DHPE are added. Lipid mixing is observed by fluorescence microscopy after the addition of the vesicles and in the presence of calcium ions as demonstrated in Fig. 2. Fig. 2 shows discrete movie frames of the Oregon Green DHPE (top panel) and Texas Red DHPE fluorescence (bottom panel). Within the first frame, the Texas Red DHPE doped vesicle approaches the membrane surface, which can be deduced from the bright spot in the focal plane of the Texas

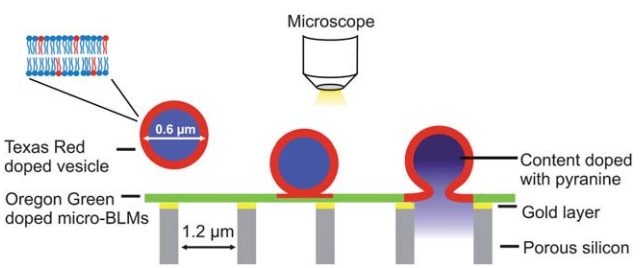

Fig. 1 Schematic drawing of the experimental setup of the fusion assay based on micro-BLMs.

Institute of Organic and Biomolecular Chemistry, Tammannstr. 2, 37077 Göttingen, Germany. E-mail: csteine@gwdg.de; Fax: +49 551 393228; Tel: +49 551 393294

† Electronic supplementary information (ESI) available: Materials and methods. See DOI: 10.1039/c0sm01429j

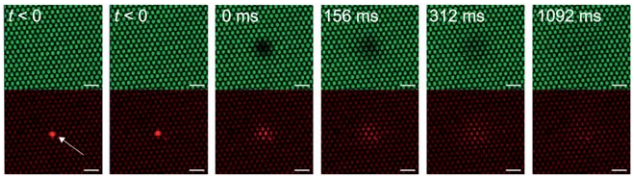

Fig. 2 Sequence of fluorescence micrographs showing a typical fusion event. The Oregon Green DHPE fluorescence of the micro-BLMs is shown in green (top panel), the Texas Red DHPE fluorescence is depicted in red (bottom panel). Lipid mixing is indicated by the distribution of the Texas Red fluorescence dye from the vesicle into the planar membrane and the simultaneous quenching of the Oregon Green DHPE fluorescence. The time zero is set arbitrarily. Scale bar: 5 μm.

Red fluorescence image. Within the second frame, the Texas Red DHPE fluorescence starts to distribute within the plane of the micro-BLM, which coincides with a quenching of the Oregon Green DHPE fluorescence at the same spot as a result of a Förster resonance energy transfer (FRET). This observation is interpreted as lipid mixing. In general, each vesicle that docks at the micro-BLM rapidly fuses as observed by lipid mixing. Such fusion events are, however, only observed in the presence of calcium ions. In the absence of Ca^{2+}, no fusion events were observed, supporting the need for Ca^{2+} as a fusogenic agent.[3,12] The observation of single fusion events enables us to distinguish between fusion events that occur on the pore rim and fusion of the vesicle with the pore-spanning area. Both cases are found to the same extent indicating that the LUVs fuse with the lipid/DPPTE hybrid bilayer as well as with the pore-spanning lipid bilayer.

For data analysis, integrated fluorescence intensities were extracted from a circular region of interest (ROI) centred on the origin of the fusion event. The radius r of the ROI was chosen manually depending on the size of the vesicle and was generally in the range of 4 μm. A characteristic time lapse of the fluorescence intensities is shown in Fig. 3. While the Texas Red fluorescence increases if the vesicle approaches the planar membrane interface, it decreases upon lipid mixing. At the same time, a sharp decrease in the Oregon Green intensity, followed by a slow re-increase, is observed as a result of FRET. We suggest that the re-increase in the Oregon Green and the decrease in the Texas Red fluorescence intensity are caused by the lipid diffusion of the Texas Red DHPE acceptor fluorophors within the micro-BLM.

To support this notion, we analyzed the fluorescence decay of the Texas Red DHPE fluorescence by means of eqn (1):[25]

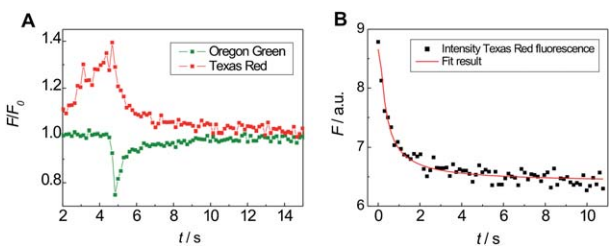

Fig. 3 (A) Time resolved changes in the relative fluorescence intensity of Oregon Green and Texas Red DHPE during a fusion event. The onset of lipid mixing is indicated by the sudden drop in the Oregon Green fluorescence intensity and the slow decrease in Texas Red fluorescence. (B) Fit of eqn (1) (solid line) to the time course of the Texas Red fluorescence intensity resulting in a diffusion coefficient of $D = (6.6 \pm 0.6)$ μm^2 s^{-1}.

$$F_{\mathrm{ROI}}(t) = AN\left[1 - \exp\left(\frac{-r^2}{4Dt}\right)\right] + F_{\mathrm{b}} \quad (1)$$

Eqn (1) is derived by solving the time-dependent diffusion equation for the release of fluorescent lipids from the vesicle into the planar bilayer at the origin of the fusion event. F_{ROI} is the Texas Red fluorescence in the ROI, N is the number of fluorescent molecules transferred from the vesicle to the micro-BLM, A is a proportionality constant that converts concentration to fluorescence intensity, and F_{b} accounts for background fluorescence. By fitting eqn (1) to the data, the diffusion coefficient D for the Texas Red DHPE molecules in the micro-BLM for every single fusion event can be obtained. An average diffusion coefficient of $D = (9 \pm 5)$ μm^2 s^{-1} ($n = 46$) was determined. This value is in very good agreement with that found for micro-BLMs composed of DPhPC on DPPTE functionalized porous silicon substrates with pore sizes of 7 μm as obtained by fluorescence recovery after photobleaching (FRAP)[26] and thus supports that indeed lipid diffusion as a result of lipid mixing is observed.

As the fusion of each individual vesicle with the planar pore-spanning membrane adds additional lipid material to the bilayer, we asked the question, if and how the excess of lipid material changes the membrane morphology. To address this question, we used scanning ion conductance microscopy (SICM),[27,28] which has been shown to be well suited to visualize pore-spanning membranes.[29]

In contrast to scanning force microscopy, which indents the pore-spanning membranes as a function of loading force,[24] SICM is contact-free and thus is expected to not manipulate the position of the membrane on the pores significantly. The SICM images reveal that the membrane covered pores appear as shallow depressions (Fig. 4A). This observation can be rationalized by the fact that the membrane is in intimate contact with the gold layer, as the membrane lipids strongly interact with the DPPTE molecules chemisorbed on the gold

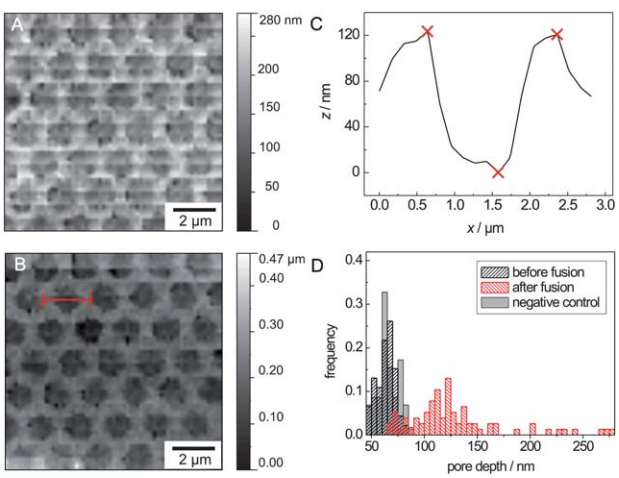

Fig. 4 Scanning ion conductance microscopy image of micro-BLMs before (A) and after (B) fusion of LUVs. The image size is 10 × 10 μm^2 with a resolution of 512 × 512 pixels. (C) Height profile of the cross-section along the red line shown in (B). The red crosses in (C) mark the positions on which the z-positions were readout to determine the height difference between pore rim and pore-spanning membrane. In this way, the depth of each pore was obtained. (D) Histogram of the depth distribution of lipid membranes spanning the pores. Before fusion the height difference ranges from 45–95 nm, while after fusion values in the regime of 65–280 nm are found.

surface. Thus, the membrane is bent into the pore, while it becomes detached and freely suspends the pore at the bottom of the gold layer. As a result, each individual membrane is positioned at a certain depth below the pore rims, which was determined to be in the range of 45–95 nm (Fig. 4D). To monitor any changes in the morphology of the membranes as a function of the occurring fusion events, SICM images were taken before (Fig. 4A) and after fusion of vesicles (Fig. 4B). The depth distribution was analyzed *via* line profiles across each individual pore. From each profile, the height difference between the pore rim and the membrane located inside the pore was readout (Fig. 4C). In all experiments, the fusion of vesicles changed the pore depth distribution to larger values (Fig. 4D). Control experiments demonstrated that incubating or rinsing the membranes with buffer does not lead to any changes in the determined pore depths (Fig. 4D). We attribute this increased pore depth as a result of fusion events to the fact that the additional lipid material is stored in the pore-spanning region of the micro-BLMs so that the membrane bulges deeper into the pore. Even though the change in depth was different for each individual experiment, which is explained by the fact that the membrane depth is determined by the number of fusion events that occur on the surface and which cannot be precisely controlled, in each experiment the depth only becomes larger after the fusion events.

In general, lipid mixing as observed by FRET is not only found if full fusion occurs but also if the fusion process is stalled on the stage of hemifusion. Even though in this case the distribution of the Texas Red DHPE fluorescence is expected to be not complete, an unambiguous assignment for full fusion would be the release of the aqueous content of the vesicle. To monitor such release, we filled the vesicles with the water soluble dye pyranine. A simultaneous measurement of lipid mixing by FRET and dye release allowed us to rule out that the vesicle or planar membrane ruptures within the observed time period. The fluorescence micrographs in Fig. 5 demonstrate that the pyranine filled vesicle approaches the membrane surface followed by an instantaneous release of the aqueous dye within about 230 ms. Simultaneously, lipid mixing occurs, which can be deduced from the FRET between the Oregon Green and Texas Red DHPE. From the time resolved change in Texas Red DHPE fluorescence, a mean diffusion coefficient of $D = (14 \pm 9)$ μm^2 s^{-1} ($n = 82$) was extracted, which is in accordance with the FRAP data and the lipid mixing experiments without pyranine. The rather large errors of the determined diffusion coefficients might reflect the different amounts of the residual solvent found in micro-BLMs as a result of the preparation procedure.

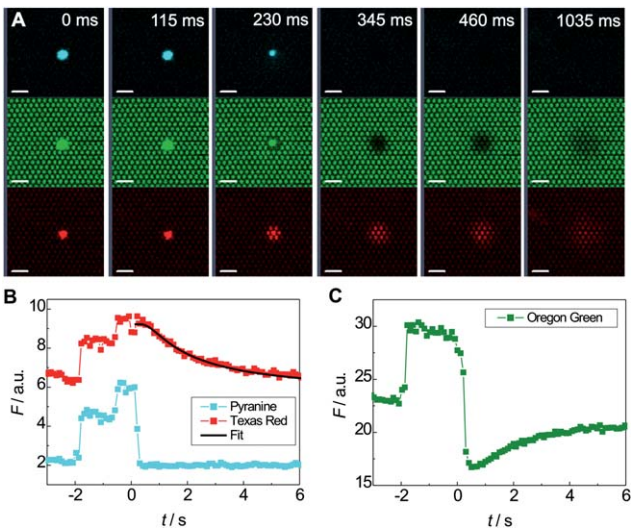

Fig. 5 (A) Fluorescence micrographs displaying a fusion event of a Texas Red DHPE doped vesicle filled with pyranine with an Oregon Green DHPE doped micro-BLM. Scale bar: 5 μm. (B) Time resolved changes in the fluorescence intensity obtained during the fusion event shown in (A) The fit of eqn (1) (solid line) to the time course of the Texas Red fluorescence intensity results in a diffusion coefficient of $D = (11 \pm 1)$ μm^2 s^{-1}.

One could still argue that the aqueous dye release is caused by vesicle leakage. Wang and coworkers reported calcein dequenching bursts during fusion within 40 ms that turned out to be caused by vesicle leakage.[6] Even though vesicle leakage cannot be ruled out completely in our case, the longer time scale of the pyranine disappearance might argue against vesicle rupturing. Moreover, the large space underneath the bilayer is expected to favour the release of dye molecules *via* a fusion pore.

In summary, we were able to show that micro-BLMs provide a stable and robust planar membrane that allows the detection of fusion events in a time resolved manner at the single vesicle level by means of time lapsed fluorescence microscopy. SICM images reveal that the lipid material is stored into the pore-spanning membrane resulting in a different membrane morphology after fusion. By entrapping a water soluble dye into the unilamellar vesicles, it became possible to not only observe lipid mixing but also the release of the aqueous content of the vesicles. As micro-BLMs are robust and long-term stable, while they are still accessible from both aqueous sides, they might pave the way to get new insights into different aspects of membrane fusion processes.

Acknowledgements

The authors thank the DFG (SFB 803) for financial support.

Notes and references

1 R. Jahn, T. Lang and T. C. Südhof, *Cell*, 2003, **112**, 519–533.
2 Y.-H. M. Chan, B. van Lengerich and S. G. Boxer, *Proc. Natl. Acad. Sci. U. S. A.*, 2009, **106**, 979–984.
3 A. Chanturiya, L. V. Chernomordik and J. Zimmerberg, *Proc. Natl. Acad. Sci. U. S. A.*, 1997, **94**, 14423–14428.
4 S. Kreye, J. Malsam and T. H. Söllner, *Methods Mol. Biol.*, 2008, **440**, 37–50.
5 G. Stengel, R. Zahn and F. Höök, *J. Am. Chem. Soc.*, 2007, **129**, 9584–9585.
6 T. Wang, E. A. Smith, E. R. Chapman and J. C. Weisshaar, *Biophys. J.*, 2009, **96**, 4122–4131.
7 L. V. Chernomordik, J. Zimmerberg and M. M. Kozlov, *J. Cell Biol.*, 2006, **175**, 201–207.
8 A. Cypionka, A. Stein, J. M. Hernandez, H. Hippchen, R. Jahn and P. J. Walla, *Proc. Natl. Acad. Sci. U. S. A.*, 2009, **106**, 18575–18580.
9 T. Y. Yoon, B. Okumus, F. Zhang, Y. K. Shin and T. Ha, *Proc. Natl. Acad. Sci. U. S. A.*, 2006, **103**, 19731–19736.
10 M. K. Domanska, V. Kiessling, A. Stein, D. Fasshauer and L. K. Tamm, *J. Biol. Chem.*, 2009, **284**, 32158–32166.
11 V. I. Razinkov, G. B. Melikyan and F. S. Cohen, *Biophys. J.*, 1999, **77**, 3144–3151.
12 A. Chanturiya, P. Scaria and M. C. Woodle, *J. Membr. Biol.*, 2000, **176**, 67–75.
13 V. A. Frolov, A. Y. Dunina-Barkovskaya, A. V. Samsonov and J. Zimmerberg, *Biophys. J.*, 2003, **85**, 1725–1733.
14 M. K. Domanska, V. Kiessling and L. K. Tamm, *Biophys. J.*, 2010, **99**, 2936–2946.

15 E. Karatekin, J. Di Giovanni, C. Iborra, J. Coleman, B. O'Shaughnessy, M. Seagar and J. E. Rothman, *Proc. Natl. Acad. Sci. U. S. A.*, 2010, **107**, 3517–3521.
16 D. L. Floyd, J. R. Ragains, J. J. Skehel, S. C. Harrison and A. M. van Oijen, *Proc. Natl. Acad. Sci. U. S. A.*, 2008, **105**, 15382–15387.
17 L. Wessels, M. W. Elting, D. Scimeca and K. Weninger, *Biophys. J.*, 2007, **93**, 526–538.
18 M. Fix, T. J. Melia, J. K. Jaiswal, J. Z. Rappoport, D. You, T. H. Söllner, J. E. Rothman and S. M. Simon, *Proc. Natl. Acad. Sci. U. S. A.*, 2004, **101**, 7311–7316.
19 C. Kepplinger, I. Höfer and C. Steinem, *Chem. Phys. Lipids*, 2009, **160**, 109–113.
20 W. Römer, Y. H. Lam, D. Fischer, A. Watts, W. B. Fischer, P. Göring, R. B. Wehrspohn, U. Gösele and C. Steinem, *J. Am. Chem. Soc.*, 2004, **126**, 16267–16274.
21 W. Römer and C. Steinem, *Biophys. J.*, 2004, **86**, 955–965.
22 E. K. Schmitt, M. Nurnabi, R. J. Bushby and C. Steinem, *Soft Matter*, 2008, **4**, 250–253.
23 E. K. Schmitt, C. Weichbrodt and C. Steinem, *Soft Matter*, 2009, **5**, 2247–2253.
24 I. Mey, M. Stephan, E. K. Schmitt, M. M. Müller, M. Ben Amar, C. Steinem and A. Janshoff, *J. Am. Chem. Soc.*, 2009, **131**, 7031–7039.
25 T. Liu, T. Wang, E. R. Chapman and J. C. Weisshaar, *Biophys. J.*, 2008, **94**, 1303–1314.
26 D. Weiskopf, E. K. Schmitt, M. H. Klühr, S. K. Dertinger and C. Steinem, *Langmuir*, 2007, **23**, 9134–9139.
27 M. Böcker, H. Fuchs and T. E. Schäffer, *Nanotechnology*, 2009, **6**, 197–211.
28 J. Rheinländer and T. E. Schäffer, *J. Appl. Phys.*, 2009, **105**, 094905.
29 M. Böcker, S. Muschter, E. K. Schmitt, C. Steinem and T. E. Schäffer, *Langmuir*, 2009, **25**, 3022–3028.